

# An Efficient Method for Quantifying the Aggregate Flexibility of Plug-in Electric Vehicle Populations

Feras Al Taha, Tyrone Vincent, Eilyan Bitar

**Abstract**—Plug-in electric vehicles (EVs) are widely recognized as being highly flexible electric loads that can be pooled and controlled via aggregators to provide low-cost energy and ancillary services to wholesale electricity markets. To participate in these markets, an aggregator must encode the aggregate flexibility of the population of EVs under their command as a single polytope that is compliant with existing market rules. To this end, we investigate the problem of characterizing the aggregate flexibility set of a heterogeneous population of EVs whose individual flexibility sets are given as convex polytopes in half-space representation. As the exact computation of the aggregate flexibility set—the Minkowski sum of the individual flexibility sets—is known to be intractable, we study the problems of computing maximum-volume inner approximations and minimum-volume outer approximations to the aggregate flexibility set by optimizing over affine transformations of a given convex polytope in half-space representation. We show how to conservatively approximate these set containment problems as linear programs that scale polynomially with the number and dimension of the individual flexibility sets. The class of approximations methods provided in this paper generalizes existing methods from the literature. We illustrate the improvement in approximation accuracy achievable by our methods with numerical experiments.

## I. INTRODUCTION

The widescale electrification of the transportation sector will present both challenges and novel opportunities for the efficient and reliable operation of the power grid. In particular, the increase in electricity demand driven by plug-in electric vehicle (EV) charging will sharply increase peak demand if left unmanaged [1]–[3]. However, a number of field studies have shown that the charging requirements of EVs are usually flexible in the sense that most EVs charging in workplace or residential settings remain connected to their chargers long after they’ve finished charging [1], [4]–[6]. This flexibility can be utilized by coordinating the charging profiles of individual EVs to minimize their collective contribution to peak load, or to provide energy and/or ancillary services to the regional wholesale electricity market [7].

This work was supported in part by the Natural Sciences and Engineering Research Council of Canada, in part by the Cornell Atkinson Center for Sustainability, in part by The Nature Conservancy, in part by the Holland Sustainability Project Trust, and in part by the Office of Naval Research via grant N00014-17-1-2697.

F. Al Taha is with the School of Electrical and Computer Engineering, Cornell University, Ithaca, NY, 14853, USA (e-mail: foa6@cornell.edu).

T. Vincent is with the Department of Electrical Engineering and Computer Science, Colorado School of Mines, Golden, CO 80401, USA (e-mail: tvincent@mines.edu).

E. Bitar is with the School of Electrical and Computer Engineering, Cornell University, Ithaca, NY, 14853, USA (e-mail: eyb5@cornell.edu).

Indeed, enabled by regulations such as FERC Order No. 2222 [8], load aggregators can pool and coordinate the control of many EVs and other distributed energy resources (DERs) to participate alongside conventional resources in the wholesale market [9]. Aggregators that wish to participate in the wholesale market must represent the individual flexibility sets of participating EVs as a single *aggregate flexibility set* that accurately captures the supply/demand capabilities of the individual EVs as a collective. Crucially, these aggregate flexibility sets must be encoded using bid/offer formats that are compliant with existing market rules. Traditionally, bid/offer formats have been structured to reflect the supply and demand characteristics of conventional generators and load serving entities. More recently, market rules have evolved to incorporate bid/offer formats that more accurately capture the dual supply and demand capabilities of battery storage systems, e.g., in form of time-varying upper and lower limits on power, ramping, and battery state-of-charge (SoC) [10], [11]. With this motivation in mind, we investigate the problem of designing efficient optimization-based methods to accurately approximate the aggregate flexibility set associated with a heterogeneous collection of individual EV flexibility sets.

### A. Related Work

The individual flexibility sets associated with a wide variety of distributed energy resources, including thermostatically controlled loads and plug-in EVs, are typically encoded as convex polytopes in half-space representation. The exact calculation of their aggregate flexibility set—the Minkowski sum of the individual flexibility sets—is known to be computationally intractable in general [12], [13]. As a result, a variety of methods have been developed to efficiently compute approximations that are subsets or supersets of the aggregate flexibility set (termed *inner* and *outer* approximations, respectively) [14], [15], [23]. A shortcoming of outer approximations is that they may contain infeasible points. Inner approximations, on the other hand, are guaranteed to only contain feasible points—a crucial property for control applications.

There are a number of papers that provide closed-form inner approximations for the aggregate flexibility set as a function of the individual load parameters [16], [17], [19], [24]. While these inner approximations are trivial to compute, they have been observed to be very conservative when there is considerable heterogeneity between the individual flexibility sets [18]. There have been a number of attempts to utilize convex optimization methods to construct more

accurate inner approximations. For example, Zhao et al. [25] approximate the aggregate flexibility set as a projection of a convex polytope.

Another group of papers provide methods to approximate the aggregate flexibility set by constructing convex inner approximations of the individual flexibility sets using specific convex geometries that permit the efficient computation of their Minkowski sum. For example, Müller et al. [20] approximate the individual flexibility sets using a specific class of zonotopes (a family of centrally symmetric polytopes), while Zhao et al. [18] utilize homothets (dilation and translation) of a user-defined convex polytope. Nazir et al. [22] provide an algorithm to internally approximate the individual flexibility sets using unions of homothets of axis-aligned hyperrectangles. An advantage of the proposed algorithm is that, in principle, it can approximate the true aggregate flexibility set (Minkowski sum) with arbitrary precision. However, ensuring high accuracy may require a large number of hyperrectangles—potentially compromising its scalability to large-scale systems.

We also note that there have been recent attempts to construct convex approximations of the aggregate flexibility set when the individual flexibility sets may be nonconvex [26], [27]. However, the approximations provided by these methods may contain infeasible points, as they are not provable inner approximations of the aggregate flexibility set.

### B. Main Contributions

In this paper, we study the problems of computing both *maximum-volume inner approximations* and *minimum-volume outer approximations* to the aggregate flexibility set by optimizing over affine transformations of a given convex polytope in half-space representation. The proposed class of approximations generalizes those considered by related methods from the literature, which either limit the class of approximating sets to homothets of a given convex polytope [18], or restrict the specification of the given polytope to zonotopic geometries [20].

The approach taken in this paper draws inspiration from the methods proposed in [18]. Using standard techniques from convex analysis, we show how to conservatively approximate the pair of maximum-volume and minimum-volume set containment problems as linear programs that scale polynomially with the number and dimension of the individual flexibility sets. By considering this more general family of approximating polytopes (i.e., affine transformations of convex polytopes), we are able to efficiently compute approximations to the aggregate flexibility set that improve upon the accuracy of those generated by the methods proposed in [18]. We provide a stylized example and conduct numerical experiments which show that the improvement in approximation accuracy is most pronounced when there is substantial heterogeneity between the individual flexibility sets.

We also note that, while we have focused on plug-in EVs as the motivating application for our analysis, the techniques developed in this paper can also be used to approximate the aggregate flexibility of other distributed

energy resources whose individual flexibility sets can be expressed or approximated by convex polytopes in half-space representation—these include thermostatically controlled loads (TCLs) [17], [28], [29], HVAC systems [30], and residential pool pumps [31].

### C. Notation

We employ the following notational conventions throughout the paper. Let  $\mathbb{R}$  and  $\mathbb{Z}$  denote the sets of real numbers and integers, respectively. Given a pair of integers  $n, m \in \mathbb{Z}$  satisfying  $n \leq m$ , we let  $[n..m] := \{n, n+1, \dots, m\}$  denote the set of integers from  $n$  to  $m$ . We denote the indicator function of set  $\mathcal{S}$  by  $\mathbb{1}\{x \in \mathcal{S}\} = 1$  if  $x \in \mathcal{S}$  and  $\mathbb{1}\{x \in \mathcal{S}\} = 0$  if  $x \notin \mathcal{S}$ . We denote the  $n \times n$  identity matrix by  $I_n$ . Given a pair of matrices  $A$  and  $B$  of appropriate dimension, we let  $(A, B)$  denote the matrix formed by stacking  $A$  and  $B$  vertically. Given a vector  $\gamma$  and matrix  $\Gamma$  of appropriate dimension, we denote an affine transformation of a set  $\mathbb{X}$  by  $\gamma + \Gamma\mathbb{X} := \{\gamma + \Gamma x \mid x \in \mathbb{X}\}$ .

### D. Paper Organization

The remainder of the paper is organized as follows. In Section II, we present the aggregate flexibility model and state the problems addressed in this paper. Linear programming-based methods to compute inner and outer approximations to the aggregate flexibility set are derived in Sections III and IV, respectively. Numerical experiments illustrating the proposed approximation methods are provided in Section V. Section VI concludes the paper.

## II. PROBLEM FORMULATION

In this section, we present the model of EV flexibility set and formulate the problem of finding volume maximizing (resp. minimizing) inner (resp. outer) approximations of an aggregate flexibility set.

We consider a system in which a load aggregator seeks to centrally manage the charging profiles of a finite population of plug-in electric vehicles (EVs) indexed by  $i \in \mathcal{N} := \{1, \dots, N\}$ . Time is assumed to be discrete with periods indexed by  $t \in \mathcal{T} := \{0, \dots, T-1\}$ . All time periods are assumed to be of equal length, which we denote by  $\delta > 0$ .

### A. EV Charging Dynamics

We let  $u_i(t)$  denote the charging rate of EV  $i \in \mathcal{N}$  at time  $t \in \mathcal{T}$ , and let the vector  $u_i := (u_i(0), \dots, u_i(T-1)) \in \mathbb{R}^T$  denote its charging profile. Given a charging profile  $u_i$ , the net energy supplied to each EV  $i \in \mathcal{N}$  is assumed to evolve according to the difference equation

$$x_i(t+1) = x_i(t) + u_i(t)\delta, \quad t \in \mathcal{T}, \quad (1)$$

where  $x_i(0) = 0$  and  $x_i(t)$  represents the net energy delivered to EV  $i$  over the previous  $t$  time periods. We denote the resulting net energy profile by the vector  $x_i =$

$(x_i(1), \dots, x_i(T)) \in \mathbb{R}^T$ , which satisfies Eq. (1) or, more concisely, the relationship

$$x_i = Lu_i,$$

where  $L \in \mathbb{R}^{T \times T}$  is a lower triangular matrix given by  $L_{ij} := \delta$  for all  $j \leq i$ . The lower triangular matrix  $L$  is invertible since the elements along its diagonal are all non-zero.

### B. Individual Flexibility Sets

We denote the set of admissible charging profiles associated with each EV  $i \in \mathcal{N}$  by

$$\mathbb{U}_i := \{u \in \mathbb{R}^T \mid u \in [\underline{u}_i, \bar{u}_i], Lu \in [\underline{x}_i, \bar{x}_i]\}. \quad (2)$$

The vectors  $\underline{u}_i \in \mathbb{R}^T$  and  $\bar{u}_i \in \mathbb{R}^T$  represent minimum and maximum power limits on the charging profile, respectively. The vectors  $\underline{x}_i \in \mathbb{R}^T$  and  $\bar{x}_i \in \mathbb{R}^T$  represent minimum and maximum energy limits on the net energy profile, respectively. Flexibility sets that can be expressed according to (2) are commonly referred to as *generalized battery models* in the literature [17], [18]. The family of battery models (2) is quite expressive. For example, it is able to capture time-varying EV power and energy constraints, net energy requirements, charging completion deadlines, and allowable/forbidden charging times that reflect an EV's connection status over time. We refer to the set of admissible charging profiles associated with an EV as its *individual flexibility set*, which is assumed to be nonempty. In Section V, we provide an explicit construction of the individual flexibility sets (2) using a standard EV charging model from the literature [1], [32].

Note that each flexibility set  $\mathbb{U}_i$  is a compact, convex polytope since it is defined as the intersection of  $4T$  closed half-spaces that form a bounded set.<sup>1</sup> It will be convenient to use a more concise expression for the individual flexibility sets given by

$$\mathbb{U}_i = \{u \in \mathbb{R}^T \mid Hu \leq h_i\},$$

where  $H := (L, -L, I_T, -I_T)$  and  $h_i := (\bar{x}_i, -\underline{x}_i, \bar{u}_i, -\underline{u}_i)$ . The representation of a polytope as the intersection of half-spaces is commonly referred to as a half-space representation (H-representation) of the polytope. In high dimensions, a H-representation of a compact, convex polytope is often preferred to its vertex representation (V-representation) where the polytope is defined as the convex hull of its vertices, because the number of half-spaces required to represent a convex polytope (at least one per facet of the polytope) is much smaller than the number of vertices needed to represent the same polytope. For example, a hyperrectangle in  $\mathbb{R}^n$  has only  $2n$  facets but  $2^n$  vertices. We will occasionally refer to polytopes in H-representation (resp. V-representation) as H-polytopes (resp. V-polytopes).

<sup>1</sup>Each flexibility set  $\mathbb{U}_i$  is bounded, because it can be expressed as the intersection of two bounded sets, i.e.,  $\mathbb{U}_i = [\underline{u}_i, \bar{u}_i] \cap L^{-1}[\underline{x}_i, \bar{x}_i]$ .

### C. Aggregate Flexibility Set

The *aggregate flexibility set* associated with a finite population of EVs can be expressed as a Minkowski sum of the individual flexibility sets given by

$$\mathbb{U} := \sum_{i \in \mathcal{N}} \mathbb{U}_i = \left\{ u \in \mathbb{R}^T \mid u = \sum_{i \in \mathcal{N}} u_i, u_i \in \mathbb{U}_i \right\}. \quad (3)$$

Without loss of generality, we assume throughout the paper that the aggregate flexibility set  $\mathbb{U}$  is a full-dimensional polytope in  $\mathbb{R}^T$ .

Note that it is NP-hard to compute the Minkowski sum of two H-polytopes [33]. And while it is easy to compute the Minkowski sum of two V-polytopes (as a V-representation), all known classes of algorithms that convert a polytope from H-representation to V-representation (vertex enumeration) and vice-versa (facet enumeration) exhibit worst-case complexities that are exponential in the polytope's number of dimensions. Since the individual flexibility sets for EVs and other distributed energy resources are typically provided as H-polytopes, calculating their aggregate flexibility set exactly is therefore computationally intractable in general.

### D. Approximating the Aggregate Flexibility Set

Recognizing the aforementioned challenges, our primary objective in this paper is to devise computationally efficient methods to compute polyhedral inner approximations (i.e., subsets) and outer approximations (i.e., supersets) of the aggregate flexibility set  $\mathbb{U}$ . More precisely, we seek polytopes  $\mathbb{P}$  and  $\mathbb{Q}$  that satisfy

$$\mathbb{P} \subseteq \mathbb{U} \subseteq \mathbb{Q}.$$

To facilitate the efficient calculation of inner and outer approximations of the aggregate flexibility set, we restrict our attention to approximating polytopes that are expressed as affine transformations<sup>2</sup> of a given H-polytope  $\mathbb{U}_0 \subseteq \mathbb{R}^T$ , i.e.,

$$\mathbb{P} = \bar{p} + P\mathbb{U}_0 \text{ and } \mathbb{Q} = \bar{q} + Q\mathbb{U}_0, \quad (4)$$

where  $\bar{p}, \bar{q} \in \mathbb{R}^T$  and  $P, Q \in \mathbb{R}^{T \times T}$ . Employing the same nomenclature as in [34], we refer to affine transformations of H-polytopes as AH-polytopes. We will refer to the H-polytope  $\mathbb{U}_0$  as the *base set*, which is assumed to be fixed throughout the paper.

Given heterogeneous individual flexibility sets  $\mathbb{U}_1, \dots, \mathbb{U}_N$ , we are interested in computing a *maximum-volume* AH-polytope  $\mathbb{P} = \bar{p} + P\mathbb{U}_0$  that is contained within the aggregate flexibility set  $\mathbb{U}$  by solving the following optimal polytope containment problem

$$\text{maximize Vol}(\mathbb{P}) \text{ subject to } \mathbb{P} = \bar{p} + P\mathbb{U}_0 \subseteq \mathbb{U}, \quad (5)$$

with respect to the optimization variables  $\bar{p} \in \mathbb{R}^T$  and  $P \in \mathbb{R}^{T \times T}$ . Here,  $\text{Vol}(\cdot)$  denotes the  $T$ -dimensional volume function (a generalization of the usual volume measure in

<sup>2</sup>Examples of affine transformations include rotation, translation, shear transformation, scaling, or combinations thereof.

three dimensions to higher dimensions). By maximizing the volume of the inner approximation, we are effectively maximizing the proportion of feasible elements belonging to the aggregate flexibility set that it contains.

We also seek a *minimum-volume* AH-polytope  $\mathbb{Q} = \bar{q} + Q\mathbb{U}_0$  that contains the aggregate flexibility set  $\mathbb{U}$  by solving the following optimal polytope containment problem

$$\text{minimize Vol}(\mathbb{Q}) \quad \text{subject to} \quad \mathbb{Q} = \bar{q} + Q\mathbb{U}_0 \supseteq \mathbb{U}, \quad (6)$$

with respect to the optimization variables  $\bar{q} \in \mathbb{R}^T$  and  $Q \in \mathbb{R}^{T \times T}$ . By minimizing the volume of the outer approximation, we seek to limit the proportion of infeasible elements that it contains. We refer to feasible solutions to problem (5) (resp. problem (6)) as *inner approximations* (resp. *outer approximations*) of the aggregate flexibility set.

The optimization problems (5) and (6) are challenging to solve for a variety of reasons. First, it is computationally intractable to exactly calculate the volume of a polytope in high dimensions [35]. Second, the polytope containment conditions in problems (5) and (6) are also computationally intractable to verify in general [33], [34]. Thus, instead of attempting to compute optimal solutions to problems (5) and (6), we pursue a slightly less ambitious goal in this paper by seeking to *conservatively approximate* problems (5) and (6) by convex programs. The convex programs that we construct in Sections III and IV are modestly-sized linear programs, which are guaranteed to generate valid inner and outer approximations of the aggregate flexibility set.

### E. Choosing the Base Set

The methods proposed in this paper rely on the a priori determination of a base set  $\mathbb{U}_0$ . Inspired by the approach taken in [18], we will restrict our attention to base sets of the form

$$\mathbb{U}_0 := \{u \in \mathbb{R}^T \mid Hu \leq h_0\}, \quad (7)$$

where the right-hand side  $h_0 := (1/N) \sum_{i \in \mathcal{N}} h_i$  is an average of the individual flexibility set parameters. This specific choice of base set is intended to approximate the collection of (potentially heterogeneous) individual flexibility sets in a balanced manner.

It was previously shown in [15, Proposition 1] that a *dilation* of this base set by a factor of  $N$  results in an outer approximation of the aggregate flexibility set, i.e.,

$$\mathbb{U} \subseteq N\mathbb{U}_0. \quad (8)$$

It is also straightforward to show that if the individual flexibility sets are identical, then this particular dilation of the given base set results in an exact expression for the aggregate flexibility set, i.e.,  $\mathbb{U} = N\mathbb{U}_0$ .

It is important to note that the base set, being defined this way, belongs to the family of *generalized battery models* defined in (2). In certain applications, it may be necessary to restrict the family of allowable transformations in (4) to those which are *structure preserving*—i.e., transformations

resulting in polytopes that are also generalized battery models. For example, independent system operators that manage wholesale electricity markets do not have the visibility or means to effectively optimize the operation of individual resources within a large aggregation. As a result, current market rules require load aggregators participating in the wholesale market to represent the collective capability of the individual resources under their control in the form of a single representative energy storage resource [10], [11].

**Definition 1** (Structure-Preserving Transformations). An affine transformation  $\mathbb{P} = \bar{p} + P\mathbb{U}_0$  is said to be *structure preserving* if the resulting polytope can be expressed in H-representation as  $\mathbb{P} = \{u \in \mathbb{R}^T \mid Hu \leq h'\}$  for some  $h' \in \mathbb{R}^{4T}$ .

Note that affine transformations defined as a translation and dilation of the base set are guaranteed to be structure preserving. To see this, let  $\mathbb{P} = \bar{p} + \alpha\mathbb{U}_0$ , where  $\alpha > 0$ . Under this transformation, it is straightforward to show that  $\mathbb{P} = \{u \in \mathbb{R}^T \mid Hu \leq \alpha h_0 + H\bar{p}\}$ .

Finally, we note that while we have adopted a specific choice of base set in Eq. (7), all of the following results provided in this paper hold for any choice of base set that is an H-polytope.

### F. A Posteriori Approximation Error Bounds

We measure a posteriori how accurately a given pair of inner and outer approximations  $(\mathbb{P}, \mathbb{Q})$  capture the aggregate flexibility set using a *volume ratio* defined by

$$\rho(\mathbb{P}, \mathbb{Q}) := \text{Vol}(\mathbb{P}) / \text{Vol}(\mathbb{Q}). \quad (9)$$

The volume ratio (9) takes values in the unit interval since  $\mathbb{P} \subseteq \mathbb{U} \subseteq \mathbb{Q}$ . In particular,  $\rho(\mathbb{P}, \mathbb{Q}) = 1$  if and only if the inner and outer approximations equal the aggregate flexibility set, i.e.,  $\mathbb{P} = \mathbb{U} = \mathbb{Q}$ , since these sets are convex polytopes. The volume ratio (9) can also be used to a posteriori lower bound the relative accuracy of a given inner approximation with respect to the aggregate flexibility set according to

$$\rho(\mathbb{P}, \mathbb{Q}) \leq \text{Vol}(\mathbb{P}) / \text{Vol}(\mathbb{U}).$$

Thus, if the volume ratio  $\rho(\mathbb{P}, \mathbb{Q})$  is close to one, then the set  $\mathbb{P}$  can be considered to be an accurate inner approximation of the aggregate flexibility set  $\mathbb{U}$ .

Although it is computationally intractable to calculate the volume of a convex polytope in high dimensions [35], the volume ratio (9) can be efficiently calculated according to

$$\rho(\mathbb{P}, \mathbb{Q}) = |\det(P)| / |\det(Q)|. \quad (10)$$

This simplification follows from the identity  $\text{Vol}(A\mathbb{X}) = |\det(A)|\text{Vol}(\mathbb{X})$  (which gives the volume of a set  $\mathbb{X} \subseteq \mathbb{R}^T$  under a linear transformation  $A \in \mathbb{R}^{T \times T}$ ), and the fact that the pair of inner and outer approximations  $(\mathbb{P}, \mathbb{Q})$  are specified as affine transformations of a *common* base set.

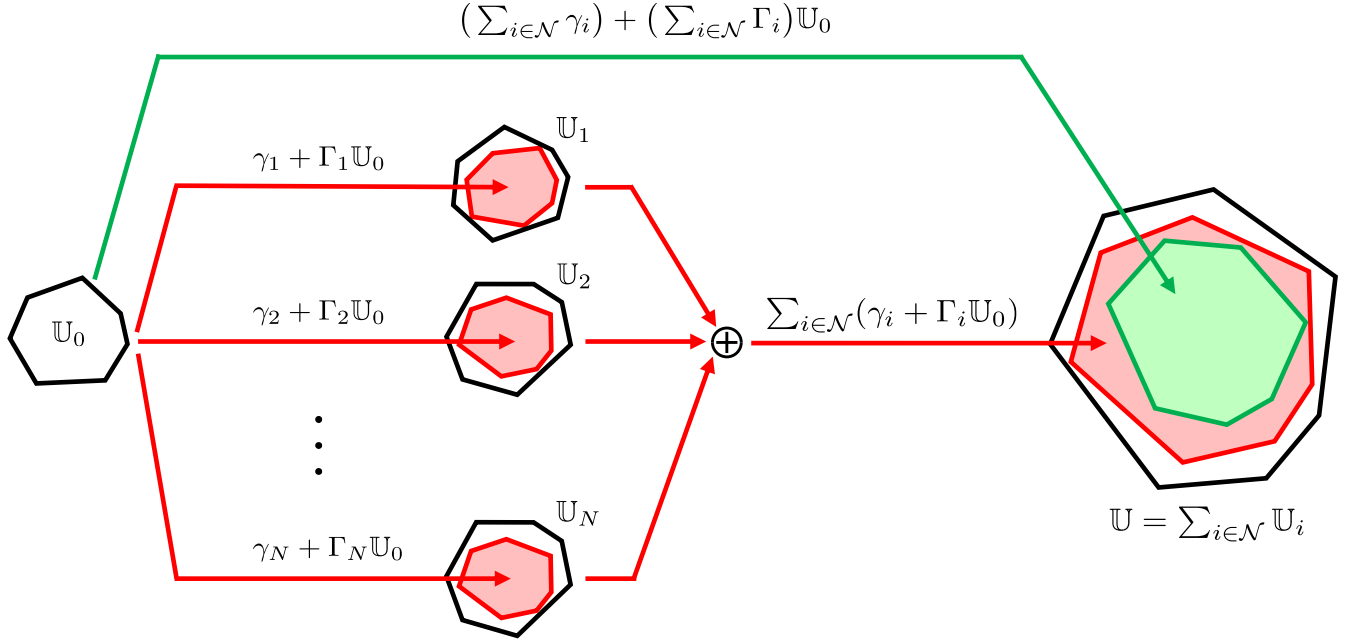


Fig. 1: Illustration of the inner approximation method proposed in this paper. Depicted are: the base set  $U_0$ ; the affine transformations  $\gamma_i + \Gamma_i U_0$  (in red) that inner approximate the individual flexibility sets  $U_i$  for  $i = 1, \dots, N$ ; and the corresponding affine transformation  $(\sum_{i \in \mathcal{N}} \gamma_i) + (\sum_{i \in \mathcal{N}} \Gamma_i) U_0$  (in green) that inner approximates the aggregate flexibility set  $U$ .

### III. INNER APPROXIMATION

In this section, we derive a linear programming approximation of the optimal inner polytope containment problem (5). We do so by constructing an inner approximation to each individual flexibility set according to:

$$\gamma_i + \Gamma_i U_0 \subseteq U_i, \quad i = 1, \dots, N. \quad (11)$$

Here,  $\gamma_i \in \mathbb{R}^T$  and  $\Gamma_i \in \mathbb{R}^{T \times T}$  ( $i = 1, \dots, N$ ) are optimization variables that will be selected to ensure that each AH-polytope  $\gamma_i + \Gamma_i U_0$  closely approximates its corresponding flexibility set  $U_i$ , while satisfying the individual set containment conditions (11), as depicted by the red arrows in the left-hand side of Fig. 1. It follows from (11) that the Minkowski sum of the resulting AH-polytopes is an inner approximation of the aggregate flexibility set, i.e.,

$$\sum_{i \in \mathcal{N}} \gamma_i + \Gamma_i U_0 \subseteq \sum_{i \in \mathcal{N}} U_i, \quad (12)$$

as illustrated by the red arrow in the right-hand side of Fig. 1. However, the Minkowski sum  $\sum_{i \in \mathcal{N}} \gamma_i + \Gamma_i U_0$  is still intractable to calculate, so instead, we sum the elements of the individual transformations to create the mapping depicted by the green arrow in the upper half of Fig. 1. This provides

an inner approximation due to the following property<sup>3</sup>

$$\left( \sum_{i \in \mathcal{N}} \gamma_i \right) + \left( \sum_{i \in \mathcal{N}} \Gamma_i \right) U_0 \subseteq \sum_{i \in \mathcal{N}} \gamma_i + \Gamma_i U_0. \quad (13)$$

Setting  $\bar{p} = \sum_{i \in \mathcal{N}} \gamma_i$  and  $P = \sum_{i \in \mathcal{N}} \Gamma_i$  yields an inner approximation to the aggregate flexibility set given by  $\mathbb{P} = \bar{p} + P U_0 \subseteq U$ , which follows from inclusions (12) and (13).

As a key building block in the construction of a convex approximation to problem (5), we provide a set of linear constraints that are necessary and sufficient for the containment of an AH-polytope within an H-polytope.

**Lemma 1** (AH-polytope in H-polytope). Let  $\mathbb{X} = \{x \in \mathbb{R}^{n_x} \mid H_x x \leq h_x\}$  and  $\mathbb{Y} = \{y \in \mathbb{R}^{n_y} \mid H_y y \leq h_y\}$ , where  $H_x \in \mathbb{R}^{m_x \times n_x}$ ,  $H_y \in \mathbb{R}^{m_y \times n_y}$ , and  $\mathbb{X}$  is assumed to be nonempty. Given a vector  $\gamma \in \mathbb{R}^{n_y}$  and matrix  $\Gamma \in \mathbb{R}^{n_y \times n_x}$ , it holds that  $\gamma + \Gamma \mathbb{X} \subseteq \mathbb{Y}$  if and only if there exists a matrix  $\Lambda \in \mathbb{R}^{m_y \times m_x}$  such that

$$\Lambda \geq 0, \quad (14)$$

$$\Lambda H_x = H_y \Gamma, \quad (15)$$

$$\Lambda h_x \leq h_y - H_y \gamma. \quad (16)$$

Lemma 1 is a known result in the literature [34], [36], [37]. It follows from standard duality results in convex analysis, and can be interpreted as a variant of Farkas' Lemma. To

<sup>3</sup>To see why the inclusion (13) is true, note that any element  $u \in (\sum_{i \in \mathcal{N}} \gamma_i) + (\sum_{i \in \mathcal{N}} \Gamma_i) U_0$  can be expressed as  $u = \sum_{i \in \mathcal{N}} (\gamma_i + \Gamma_i u_0)$  for some  $u_0 \in U_0$ . Since the element  $\gamma_i + \Gamma_i u_0$  belongs to the set  $\gamma_i + \Gamma_i U_0$  for each  $i \in \mathcal{N}$ , it follows that  $u \in \sum_{i \in \mathcal{N}} (\gamma_i + \Gamma_i U_0)$ .

keep the paper self contained, we include a simple proof that uses the strong duality property of linear programs.

*Proof.* First, notice that the set inclusion  $\gamma + \Gamma\mathbb{X} \subseteq \mathbb{Y}$  holds if and only if the AH-polytope  $\gamma + \Gamma\mathbb{X}$  is contained in each half-space defining the H-polytope  $\mathbb{Y}$ , i.e.,

$$\sup_{x \in \mathbb{X}} H_{y,j}^\top (\gamma + \Gamma x) \leq h_{y,j}, \quad j = 1, \dots, m_y, \quad (17)$$

where  $H_{y,j}^\top$  denotes the  $j$ -th row of the matrix  $H_y$  and  $h_{y,j}$  denotes the  $j$ -th element of vector  $h_y$ . Note that, for  $j = 1, \dots, m_y$ , (17) is equivalent to

$$\begin{aligned} h_{y,j} - H_{y,j}^\top \gamma &\geq \sup_{x \in \mathbb{R}^{n_x}} \{H_{y,j}^\top \Gamma x \mid H_x x \leq h_x\}, \\ \Leftrightarrow h_{y,j} - H_{y,j}^\top \gamma &\geq \inf_{\lambda_j \in \mathbb{R}_+^{m_x}} \{\lambda_j^\top h_x \mid H_x^\top \lambda_j = \Gamma^\top H_{y,j}\}, \\ \Leftrightarrow \exists \lambda_j \in \mathbb{R}_+^{m_x} \text{ s.t. } &\lambda_j^\top h_x \leq h_{y,j} - H_{y,j}^\top \gamma, H_x^\top \lambda_j = \Gamma^\top H_{y,j}. \end{aligned}$$

The equivalence in the second line follows from the strong duality of linear programs, as the primal problem (in the first line) has a nonempty feasible set. By defining  $\Lambda := (\lambda_1^\top, \dots, \lambda_{m_y}^\top)$ , the conditions in the third line can be shown to be equivalent to conditions (14), (15), and (16), which proves the desired result.  $\square$

Lemma 1 can be used to linearly encode the individual set containment conditions  $\gamma_i + \Gamma_i \mathbb{U}_0 \subseteq \mathbb{U}_i$  ( $i = 1, \dots, N$ ). Using this linear reformulation of the individual set containment conditions in combination with property (13), we arrive at the following set of sufficient conditions for the original set containment constraint  $\bar{p} + P\mathbb{U}_0 \subseteq \mathbb{U}$ .

**Theorem 2** (AH-polytope in Sum of H-polytopes). It holds that  $\bar{p} + P\mathbb{U}_0 \subseteq \mathbb{U}$  if there exist  $\gamma_i \in \mathbb{R}^T$ ,  $\Gamma_i \in \mathbb{R}^{T \times T}$ , and  $\Lambda_i \in \mathbb{R}^{4T \times 4T}$  for  $i = 1, \dots, N$  such that

$$[\bar{p}, P] = \sum_{i=1}^N [\gamma_i, \Gamma_i], \quad (18)$$

$$\Lambda_i \geq 0, \quad i = 1, \dots, N, \quad (19)$$

$$\Lambda_i H = H \Gamma_i, \quad i = 1, \dots, N, \quad (20)$$

$$\Lambda_i h_0 \leq h_i - H \gamma_i, \quad i = 1, \dots, N. \quad (21)$$

The sufficient conditions provided in Theorem 2 are linear with respect to the variables  $\bar{p}$ ,  $P$ ,  $\gamma_i$ ,  $\Gamma_i$ , and  $\Lambda_i$  ( $i = 1, \dots, N$ ). As a result, the set containment constraint  $\bar{p} + P\mathbb{U}_0 \subseteq \mathbb{U}$  can be conservatively approximated by a finite set of linear constraints in these variables, where the resulting number of decision variables and constraints scales polynomially with the size of the input data.

*Proof.* It follows from Lemma 1 that, for each  $i \in \mathcal{N}$ , conditions (19), (20), and (21) are necessary and sufficient for the set inclusion  $\gamma_i + \Gamma_i \mathbb{U}_0 \subseteq \mathbb{U}_i$ . Hence,

$$\sum_{i \in \mathcal{N}} \gamma_i + \Gamma_i \mathbb{U}_0 \subseteq \sum_{i \in \mathcal{N}} \mathbb{U}_i = \mathbb{U}.$$

The desired result then follows from (13) and (18) which together imply that  $\bar{p} + P\mathbb{U}_0 \subseteq \sum_{i \in \mathcal{N}} \gamma_i + \Gamma_i \mathbb{U}_0$ .  $\square$

With the conservative linear approximation of the containment constraint  $\bar{p} + P\mathbb{U}_0 \subseteq \mathbb{U}$  provided by Theorem 2 in hand,

we now turn to the problem of approximating the optimal inner polytope containment problem (5) by a linear program under structure-preserving affine transformations in Section III-A, and general affine transformations in Section III-B.

#### A. Structure-Preserving Transformations

We first consider a family of *structure-preserving transformations* obtained by a translation and positive scaling of the base set:

$$\mathbb{P} = \bar{p} + \alpha \mathbb{U}_0,$$

where  $\alpha > 0$  denotes the scaling factor. Given this restriction on the family of allowable transformations, the volume of the inner approximating polytope  $\mathbb{P}$  can be expressed as  $\text{Vol}(\mathbb{P}) = |\det(\alpha I_T)| \text{Vol}(\mathbb{U}_0) = \alpha^T \text{Vol}(\mathbb{U}_0)$ . Since the base set  $\mathbb{U}_0$  is assumed to be fixed throughout the paper, maximizing the volume of  $\mathbb{P}$  is equivalent to maximizing the scaling factor  $\alpha$ . Using this fact in combination with the sufficient containment conditions provided by Theorem 2, we arrive at the following conservative approximation of the original optimal inner polytope containment problem (5):

$$\begin{aligned} &\text{maximize} && \alpha \\ &\text{subject to} && [\bar{p}, \alpha I_T] = \sum_{i=1}^N [\gamma_i, \Gamma_i], \\ &&& \alpha > 0, \\ &&& \Lambda_i \geq 0, \quad i = 1, \dots, N, \\ &&& \Lambda_i H = H \Gamma_i, \quad i = 1, \dots, N, \\ &&& \Lambda_i h_0 \leq h_i - H \gamma_i, \quad i = 1, \dots, N. \end{aligned} \quad (22)$$

Problem (22) is a linear program (LP) in the decision variables  $\bar{p}$ ,  $\alpha$ ,  $\gamma_i$ ,  $\Gamma_i$ , and  $\Lambda_i$  ( $i = 1, \dots, N$ ).

**Remark 1** (Comparison to the method in [18]). We briefly remark on the relationship between the structure-preserving LP approximation provided in (22) and a related class of structure-preserving LP approximations proposed by Zhao *et al.* [18]. At their core, both methods apply affine transformations to the given base set to construct inner approximations to the individual flexibility sets, the Minkowski sum of which yields an inner approximation to the aggregate flexibility set. The methods diverge in terms of the class of affine transformations used to construct these approximations. Specifically, Zhao *et al.* [18] restricts the class of affine transformations to homothets (dilation and translation) of the given base set, while our approach utilizes a more general class of affine transformations.

More precisely, the method provided in [18] entails finding a maximal inner approximation to each individual flexibility set by solving the following problem for every  $i \in \mathcal{N}$ :

$$\text{maximize } \alpha_i \text{ subject to } \gamma_i + \alpha_i \mathbb{U}_0 \subseteq \mathbb{U}_i. \quad (23)$$

The decision variables are the translation  $\gamma_i \in \mathbb{R}$  and scaling  $\alpha_i \in \mathbb{R}$  parameters associated with each homothet  $i \in \mathcal{N}$ . The resulting collection of homothets are then summed to yield a structure-preserving inner approximation to the aggregate flexibility set given by the AH-polytope  $(\sum_{i \in \mathcal{N}} \gamma_i) + (\sum_{i \in \mathcal{N}} \alpha_i) \mathbb{U}_0$ . Clearly, the restriction

to homothetic transformations in (23) will result in overly conservative approximations if the individual flexibility sets differ significantly in shape or dimension from the base set  $\mathbb{U}_0$ . This limitation is perhaps most pronounced in settings where an individual flexibility set has lower dimension than the base set (i.e.,  $\dim \mathbb{U}_i < \dim \mathbb{U}_0$ ). In such settings, the only feasible homothetic transformations satisfying the containment constraint in (23) are those having a zero scaling factor  $\alpha_i = 0$ , resulting in internal approximations that are singletons.

The structure-preserving approximation method provided in this paper addresses the aforementioned shortcomings by enabling the optimization over general affine transformations of the base set of the form  $\gamma_i + \Gamma_i \mathbb{U}_0$  ( $i = 1, \dots, N$ ), requiring only that the resulting AH-polytope  $(\sum_{i \in \mathcal{N}} \gamma_i) + (\sum_{i \in \mathcal{N}} \Gamma_i) \mathbb{U}_0$  be structure preserving by enforcing the constraint  $\sum_{i \in \mathcal{N}} \Gamma_i = \alpha I_T$ . This enlargement of the set of structure-preserving approximations afforded by our method can significantly improve upon the quality of inner approximations to the aggregate flexibility set when the individual flexibility sets are heterogeneous in shape. In Figure 2, we provide a two-dimensional example that clearly illustrates the advantages of our method in comparison to the method proposed by Zhao *et al.* [18]. By using a non-uniform scaling of the base set to approximate each of the individual flexibility sets, our method generates an inner approximation to the aggregate flexibility set (depicted in green) that substantially improves upon the inner approximation produced by the method of Zhao *et al.* (depicted in blue). We also draw a comparison using more extensive numerical experiments in Section V-C.

Finally, we note that the method of Zhao *et al.* [18] is parallelizable in nature, requiring the solution of  $N$  separate LPs (one for each flexibility set) with  $O(T^2)$  decision variables each. In contrast, our structure-preserving inner approximation method requires the solution of a single larger LP (22) with  $O(NT^2)$  decision variables due to the coupling constraint  $\sum_{i \in \mathcal{N}} \Gamma_i = \alpha I_T$ .

### B. General Affine Transformations

We now show how to conservatively approximate the original optimal inner polytope containment problem (5) by a linear program when considering more general affine transformations of the base set. First, note that the volume of the transformation  $\mathbb{P} = \bar{p} + P \mathbb{U}_0$  is given by  $\text{Vol}(\mathbb{P}) = |\det(P)| \text{Vol}(\mathbb{U}_0)$ . Hence, maximizing  $\text{Vol}(\mathbb{P})$  is equivalent to maximizing  $|\det(P)|$ . As this function is nonconcave over the set of real square matrices, we linearize  $|\det(P)|$  using a first-order Taylor expansion about the identity matrix to obtain:

$$\text{Vol}(\mathbb{P}) \propto |\det(P)| \approx \text{Tr}(P) + \text{constant}. \quad (24)$$

Here, we have used the fact that, for nonsingular matrices  $P$ , the gradient of  $|\det(P)|$  with respect to  $P$  is given by  $\nabla_P |\det(P)| = |\det(P)|(P^{-1})^\top$ .

Employing the sufficient containment condition provided by Theorem 2 in combination with the linear approximation of the volume objective function in (24) leads to the following conservative approximation of the original optimal inner polytope containment problem (5):

$$\begin{aligned} & \text{maximize} && \text{Tr}(P) \\ & \text{subject to} && [\bar{p}, P] = \sum_{i=1}^N [\gamma_i, \Gamma_i], \\ & && \Lambda_i \geq 0, \quad i = 1, \dots, N, \\ & && \Lambda_i H = H \Gamma_i, \quad i = 1, \dots, N, \\ & && \Lambda_i h_0 \leq h_i - H \gamma_i, \quad i = 1, \dots, N. \end{aligned} \quad (25)$$

Problem (25) is a LP in the decision variables  $\bar{p}$ ,  $P$ ,  $\gamma_i$ ,  $\Gamma_i$ , and  $\Lambda_i$  ( $i = 1, \dots, N$ ).

Note that problem (25) reduces to the structure-preserving LP (22) under the additional convex restriction that  $P = \alpha I_T$  and  $\alpha > 0$ . In Section V, we conduct numerical experiments illustrating the improvement in approximation accuracy achievable by optimizing over the more general family of affine transformations encoded in problem (25). This improvement in approximation accuracy is also illustrated pictorially in the two-dimensional example provided in Figure 2, where the inner approximation produced by the LP in (25) is depicted in red.

**Remark 2** (Decomposition). It is important to note that, unlike the structure-preserving LP (22), problem (25) possesses *block-separable structure* in the variables  $\gamma_i$ ,  $\Gamma_i$ , and  $\Lambda_i$  ( $i = 1, \dots, N$ ). This structure can be exploited to decompose problem (25) into  $N$  separate LPs given by

$$\begin{aligned} & \text{maximize} && \text{Tr}(\Gamma_i) \\ & \text{subject to} && \Lambda_i \geq 0, \\ & && \Lambda_i H = H \Gamma_i, \\ & && \Lambda_i h_0 \leq h_i - H \gamma_i, \end{aligned} \quad (26)$$

for  $i = 1, \dots, N$ . Geometrically, the LPs in this decomposition are equivalent to

$$\text{maximize } \text{Tr}(\Gamma_i) \quad \text{subject to } \gamma_i + \Gamma_i \mathbb{U}_0 \subseteq \mathbb{U}_i \quad (27)$$

for  $i = 1, \dots, N$ . The equivalence between problems (26) and (27) follows from Lemma 1. Crucially, these LPs can be solved sequentially or in parallel, producing an optimal solution to the original problem (25) via the reconstruction  $[\bar{p}, P] = \sum_{i=1}^N [\gamma_i, \Gamma_i]$ .

We close this section by reminding the reader that the proposed LP approximation (25) is based on a linearization of the volume objective function about the identity matrix. It may be possible to improve upon the quality of solutions generated by this approximation by using an iterative linearization-maximization method to locally maximize the given objective function [38]. We leave this as a direction for future work.

### C. Disaggregation

To implement a given aggregate power profile  $u \in \mathbb{U}$  in the aggregate flexibility set, the load aggregator must

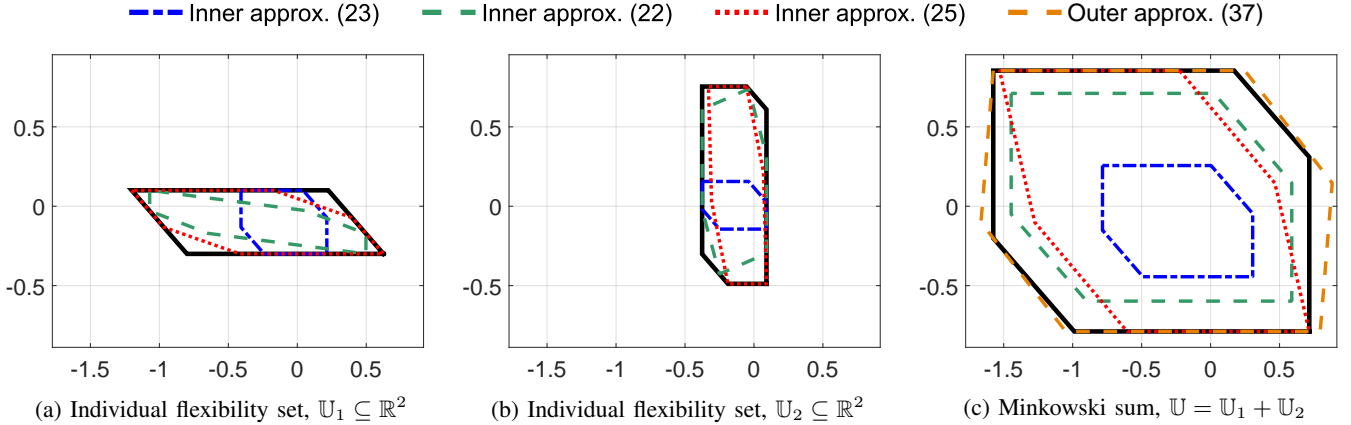


Fig. 2: Comparison of inner and outer approximation methods. (a), (b) Two individual flexibility sets  $\mathbb{U}_i = \{x \mid Hx \leq h_i\}$  ( $i = 1, 2$ ) with randomly sampled right-hand side vectors and (c) their Minkowski sum  $\mathbb{U} = \mathbb{U}_1 + \mathbb{U}_2$  are depicted as black solid lines.

disaggregate that element into a finite collection of individual power profiles that can be feasibly executed by each EV in the given population. This corresponds to finding a collection of points  $u_i \in \mathbb{U}_i$  for  $i = 1, \dots, N$  such that  $u = \sum_{i \in \mathcal{N}} u_i$ . Of course, this particular approach to disaggregation corresponds to solving a linear feasibility problem whose size grows with the number of EVs in the population.

Alternatively, using the class of inner approximations provided in this paper, one can obtain feasible disaggregated power profiles without having to solve such linear programs. Specifically, the computation of an inner approximation according to the conditions in Theorem 2 yields—as a byproduct—an affine mapping that can transform any feasible point in the inner approximation into a collection of individually feasible points.

To better understand this approach to disaggregation, let  $\mathbb{P} = \bar{p} + P\mathbb{U}_0 \subseteq \mathbb{U}$  denote an inner approximation to the aggregate flexibility set satisfying conditions (18)-(21) in Theorem 2, and let  $u \in \mathbb{P}$  denote an arbitrary point in this set. It follows from (18) that there exists a point  $u_0 \in \mathbb{U}_0$  such that the given point  $u$  can be expressed as

$$u = \bar{p} + Pu_0 = \sum_{i \in \mathcal{N}} \gamma_i + \Gamma_i u_0. \quad (28)$$

Additionally, it follows from conditions (19)-(21) that  $\gamma_i + \Gamma_i \mathbb{U}_0 \subseteq \mathbb{U}_i$  for all  $i \in \mathcal{N}$  (a direct consequence of Lemma 1). This implies that  $\gamma_i + \Gamma_i u_0 \in \mathbb{U}_i$  for all  $i \in \mathcal{N}$ . Thus, the given point  $u \in \mathbb{P}$  can be disaggregated into a collection of individually feasible points given by

$$u_i := \gamma_i + \Gamma_i u_0 \quad (29)$$

for  $i = 1, \dots, N$ . Finally, note that if the matrix  $P$  is also invertible, then the disaggregated power profiles in (29) can

be expressed as explicit functions of the aggregate power profile  $u$  as follows:

$$u_i := \gamma_i + \Gamma_i P^{-1}(u - \bar{p}) \quad (30)$$

for  $i = 1, \dots, N$ . We illustrate this approach to disaggregation using a numerical example in Section V-B.

#### IV. OUTER APPROXIMATION

In this section, we build upon the results of Section III to construct a LP approximation of the optimal outer polytope containment problem (6). In Section V, we utilize the resulting outer approximation to estimate the relative accuracy of a given inner approximation with respect to the aggregate flexibility set using the volume ratio defined in (9).

Fig. 3 summarizes the outer approximation method proposed in this paper. Our approach is based on the construction of separate outer approximations to each of the individual flexibility sets of the form:

$$\beta_i + \frac{1}{N} Q\mathbb{U}_0 \supseteq \mathbb{U}_i, \quad i = 1, \dots, N, \quad (31)$$

where  $\beta_i \in \mathbb{R}^T$  ( $i = 1, \dots, N$ ) and  $Q \in \mathbb{R}^{T \times T}$  are optimization variables. The outer approximations to the individual flexibility sets are based on an identical linear transformation to enable the calculation of their Minkowski sum in closed form. From (31), summing the individual outer approximations yields an outer approximation to the aggregate flexibility set given by

$$\sum_{i \in \mathcal{N}} \left( \beta_i + \frac{1}{N} Q\mathbb{U}_0 \right) = \left( \sum_{i \in \mathcal{N}} \beta_i \right) + Q\mathbb{U}_0 \supseteq \sum_{i \in \mathcal{N}} \mathbb{U}_i.$$

Setting  $\bar{q} = \sum_{i \in \mathcal{N}} \beta_i$ , we obtain the desired outer approximation  $\mathbb{Q} = \bar{q} + Q\mathbb{U}_0 \supseteq \mathbb{U}$ .

Based on this construction, the following result builds upon Lemma 1 to provide a set of sufficient conditions for the containment constraint  $\mathbb{U} \subseteq \bar{q} + Q\mathbb{U}_0$ .



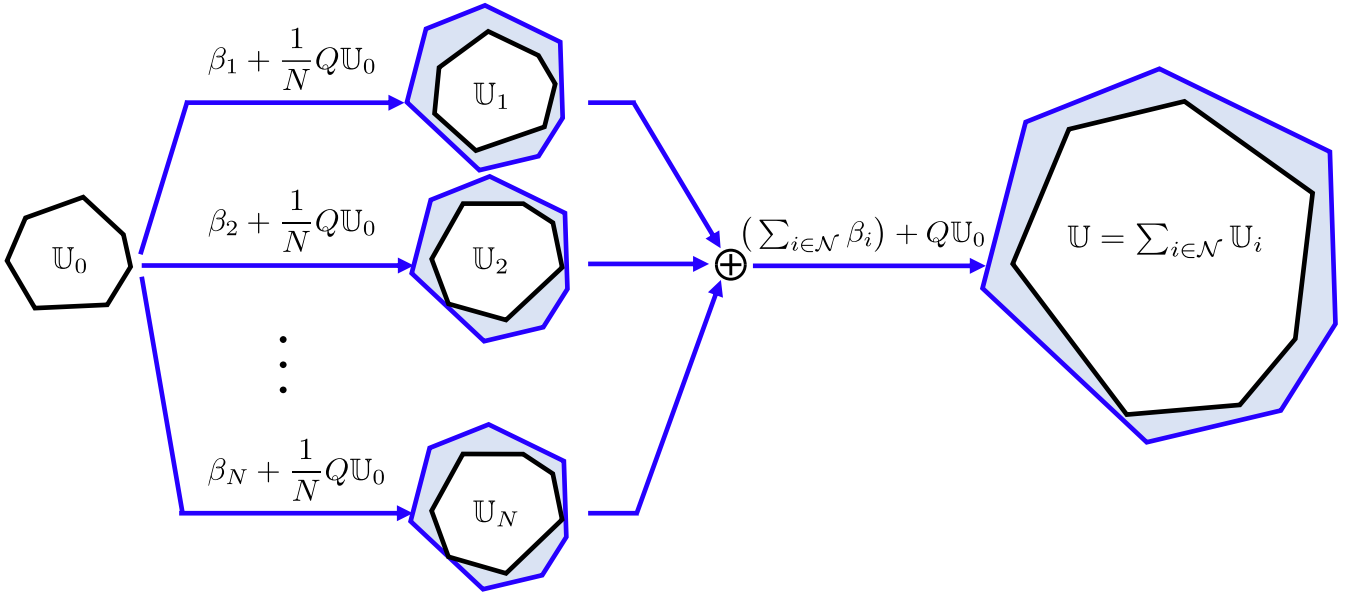


Fig. 3: Illustration of the outer approximation method proposed in this paper. Depicted are: the base set  $U_0$ ; the affine transformations  $\beta_i + \frac{1}{N}QU_0$  (in blue) that outer approximate the individual flexibility sets  $U_i$  for  $i = 1, \dots, N$ ; and the corresponding affine transformation  $(\sum_{i \in \mathcal{N}} \beta_i) + QU_0$  (in blue) that outer approximates the aggregate flexibility set  $U$ .

**Theorem 3** (Sum of H-polytopes in AH-polytope). It holds that  $U \subseteq \bar{q} + QU_0$  if there exist  $\Gamma \in \mathbb{R}^{T \times T}$ ,  $\gamma_i \in \mathbb{R}^T$ , and  $\Lambda_i \in \mathbb{R}^{4T \times 4T}$  for  $i = 1, \dots, N$  such that

$$\bar{q} = -Q \sum_{i=1}^N \gamma_i, \quad (32)$$

$$I_T = Q\Gamma, \quad (33)$$

$$\Lambda_i \geq 0, \quad i = 1, \dots, N, \quad (34)$$

$$\Lambda_i H = H\Gamma, \quad i = 1, \dots, N, \quad (35)$$

$$\Lambda_i h_i \leq \frac{1}{N} h_0 - H\gamma_i, \quad i = 1, \dots, N. \quad (36)$$

*Proof.* It follows from Lemma 1 that, for each  $i \in \mathcal{N}$ , conditions (34), (35) and (36) are necessary and sufficient for the set inclusion  $\gamma_i + \Gamma U_i \subseteq \frac{1}{N}U_0$ . By left multiplying both sides of this containment constraint by the matrix  $Q$ , applying the substitution (33), and rearranging terms, we obtain  $U_i \subseteq -Q\gamma_i + \frac{1}{N}QU_0$ . Summing both sides of this containment condition over  $i$ , it follows that

$$\sum_{i \in \mathcal{N}} U_i \subseteq \left( \sum_{i \in \mathcal{N}} -Q\gamma_i \right) + QU_0 = \bar{q} + QU_0,$$

where the equality follows from condition (32), completing the proof.  $\square$

In Theorem 3, the translation vectors associated with the individual flexibility set outer approximations (which are depicted in Fig. 3) are given by  $\beta_i = -Q\gamma_i$  for  $i = 1, \dots, N$ . Also, the sufficient conditions provided in Theorem 3 contain terms that are bilinear with respect to the variables  $Q$ ,  $\Gamma$  and  $\gamma_i$  ( $i = 1, \dots, N$ ). As a result, these conditions cannot be directly used to recast the optimal outer polytope containment problem as a convex program. The following result shows how to sidestep this nonconvexity by restricting the class

of allowable transformations to those which are invertible linear functions of the base set (i.e.,  $Q = QU_0$  where  $Q$  is an invertible matrix).

**Corollary 1.** Let  $Q \in \mathbb{R}^{T \times T}$  be an invertible matrix. It holds that  $U \subseteq QU_0$  if there exist  $\gamma_i \in \mathbb{R}^T$  and  $\Lambda_i \in \mathbb{R}^{4T \times 4T}$  for  $i = 1, \dots, N$  such that

$$0 = \sum_{i=1}^N \gamma_i,$$

$$\Lambda_i \geq 0, \quad i = 1, \dots, N,$$

$$\Lambda_i H = HQ^{-1}, \quad i = 1, \dots, N,$$

$$\Lambda_i h_i \leq \frac{1}{N} h_0 - H\gamma_i, \quad i = 1, \dots, N.$$

*Proof.* This result follows from Theorem 3 by setting  $\bar{q} = 0$  and left-multiplying (32) and (33) by  $Q^{-1}$ .  $\square$

The sufficient conditions provided in Corollary 1 are linear with respect to the variables  $Q^{-1}$ ,  $\Lambda_i$ , and  $\gamma_i$  ( $i = 1, \dots, N$ ). To obtain a convex conservative approximation of the containment constraint  $U \subseteq QU_0$ , it suffices to impose the conditions in Corollary 1 alongside additional convex constraints ensuring the invertibility of  $Q$ . We do so by introducing a change of variables  $Z = Q^{-1}$  and requiring that  $Z$  be a *strictly diagonally dominant* matrix with positive diagonal entries (i.e.,  $Z_{ii} > \sum_{j \neq i} |Z_{ij}|$  for  $i = 1, \dots, T$ ), which is sufficient to ensure invertibility. We also linearize the original volume objective using a first-order Taylor expansion about the identity matrix to obtain:

$$\text{Vol}(Q) \propto |\det(Z^{-1})| \approx -\text{Tr}(Z) + \text{constant}.$$

Using these approximations, we arrive at the following convex conservative approximation of the original optimal outer polytope containment problem (6):

$$\begin{aligned}
& \text{maximize} && \text{Tr}(Z) \\
& \text{subject to} && 0 = \sum_{i=1}^N \gamma_i, \\
& && \Lambda_i \geq 0, \quad i = 1, \dots, N, \\
& && \Lambda_i H = HZ, \quad i = 1, \dots, N, \\
& && \Lambda_i h_i \leq \frac{1}{N} h_0 - H\gamma_i, \quad i = 1, \dots, N, \\
& && Z_{ii} \geq \epsilon + \sum_{j \neq i} |Z_{ij}|, \quad i = 1, \dots, T.
\end{aligned} \tag{37}$$

Here,  $\epsilon > 0$  is a suitably chosen small positive constant ensuring *strict* diagonal dominance of the matrix  $Z$ , without having to enforce a strict inequality in the constraints.

Problem (37) is a convex program in the decision variables  $Z$ ,  $\gamma_i$ , and  $\Lambda_i$  ( $i = 1, \dots, N$ )—in fact, it can be recast as a linear program [39]. Problem (37) yields outer approximations to the aggregate flexibility set of the form

$$\mathbb{U} \subseteq Z^{-1}\mathbb{U}_0.$$

Figure 2(c) depicts the outer approximation to aggregate flexibility set generated by (37) (depicted in orange) using a simple two-dimensional example.

## V. EXPERIMENTS

In this section, we illustrate the approximation methods proposed in this paper using simulated EV charging requirements that are reflective of residential overnight charging scenarios. First, we show how to encode the individual charging requirements of a plug-in EV in the form of a *generalized battery model* originally defined in (2). Using this model as the basis for our simulations, we compare the approximation accuracy of the methods provided in this paper to the methods in [18].

### A. EV Charging Model

We consider a setting where each EV  $i \in \mathcal{N}$  is available to charge for a contiguous set of time periods between a plug-in time  $a_i \in \mathcal{T}$  and charging completion deadline  $d_i \in \mathcal{T}$ . For all time periods  $t \in [a_i .. d_i]$ , we assume that EV  $i$  can be charged or discharged at any rate between minimum and maximum rates,  $u_i^{\min} \in \mathbb{R}$  and  $u_i^{\max} \in \mathbb{R}$ , respectively, where  $u_i^{\min} < u_i^{\max}$ . For all time periods  $t \notin [a_i .. d_i]$ , the charging rate is required to be zero. Together, these charging profile constraints can be encoded as a generalized battery model (2) by specifying the charging profile limits  $(\bar{u}_i, \underline{u}_i)$  according to

$$\bar{u}_i(t) = u_i^{\max} \cdot \mathbb{1}\{t \in [a_i .. d_i]\} \tag{38}$$

$$\underline{u}_i(t) = u_i^{\min} \cdot \mathbb{1}\{t \in [a_i .. d_i]\} \tag{39}$$

for  $t = 0, \dots, T - 1$ . Additionally, each EV  $i$  is assumed to have a finite energy storage capacity  $x_i^{\max} \in \mathbb{R}_+$ , an initial state of charge  $x_i^{\text{init}} \in \mathbb{R}_+$  when plugging in to charge, and a desired final state of charge  $x_i^{\text{fin}} \in \mathbb{R}_+$  that must be satisfied

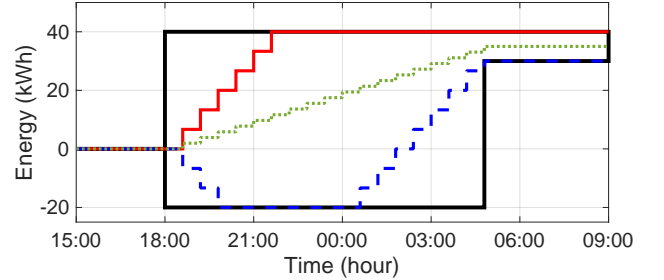
by its charging completion deadline. These constraints on the net energy profile can also be represented in a manner that is consistent with the model (2) by specifying the net energy profile limits  $(\bar{x}_i, \underline{x}_i)$  according to

$$\bar{x}_i(t) = (x_i^{\max} - x_i^{\text{init}}) \cdot \mathbb{1}\{t \geq a_i\} \tag{40}$$

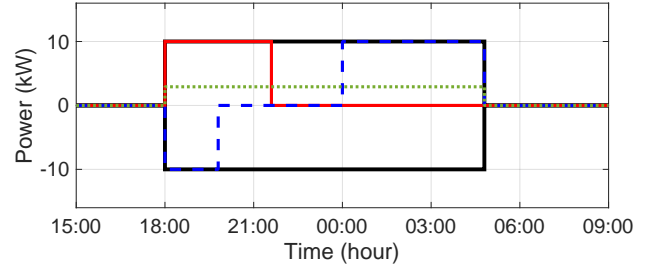
$$\underline{x}_i(t) = x_i^{\text{fin}} \cdot \mathbb{1}\{t > d_i\} - x_i^{\text{init}} \cdot \mathbb{1}\{t \geq a_i\} \tag{41}$$

for  $t = 1, \dots, T$ . Collectively, Eqs. (38)-(41) completely define the individual flexibility set of each EV  $i \in \mathcal{N}$  as a generalized battery model. We depict an example of an individual EV flexibility set in Fig. 4 using the power and energy profile limits specified in Eqs. (38)-(41). We remind the reader that the energy limits are bounds on the *net energy* delivered to the EV. For example, in Fig. 4, the EV has a battery capacity of 60 kWh and an initial state-of-charge of 20 kWh. As a result, the minimum and maximum net energy that can be supplied to the EV are -20 kWh and 40 kWh, respectively, as depicted Fig. 4(a).

Table I summarizes the EV charging parameters used in the following numerical experiments. The listed parameters are either fixed at the specified value or sampled uniformly at random from the specified interval. All of the random variables used in the experiments are assumed to be mutually independent.



(a) Net energy profiles and constraints



(b) Power profiles and constraints

Fig. 4: Example of an individual EV flexibility set. The power and net energy profile constraints are depicted as solid black lines. Three different feasible power profiles and net energy profiles are depicted as dashed-blue, solid-red, and dotted-green lines. The EV charging parameters used to construct this set are:  $\delta = 2/3$  hour,  $T = 18$  periods,  $a_i = 6$  PM,  $d_i = 5$  AM,  $u_i^{\max} = -u_i^{\min} = 10$  kW,  $x_i^{\max} = 60$  kWh,  $x_i^{\text{init}} = 20$  kWh, and  $x_i^{\text{fin}} = 50$  kWh.

Param.	Description	Value or Range
$\delta$	Time period length	2/3 hr (Sec.V-B), 1 hr (Sec.V-C)
$T$	Number of time periods	30 (Sec.V-B), 12 (Sec.V-C)
$a_i$	Plug-in time	[3 PM, 8 PM]
$d_i$	Charging deadline	[5 AM, 11 AM]
$x_i^{\max}$	Battery capacity	70 kWh
$u_i^{\max}$	Max charging rate	10 kW
$u_i^{\min}$	Min charging rate	-10 kW
$x_i^{\text{init}}$	Initial state-of-charge	14 kWh
$x_i^{\text{fin}}$	Final state-of-charge	$40 + [-30\sigma, 30\sigma]$ kWh

TABLE I: Summary of EV charging parameters used in numerical experiments. The parameters are either fixed at the specified value or uniformly distributed random variables over the specified interval. The parameter  $\sigma \in [0, 1]$  is used to control the degree of heterogeneity between the individual flexibility sets.

### B. Structure-Preserving Inner and Outer Approximations

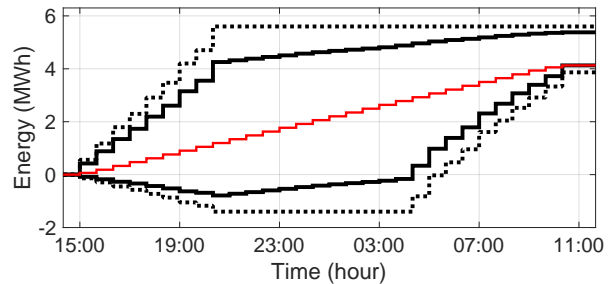
In this section, we visualize the structure-preserving inner and outer approximations generated by the methods provided in this paper. First, we randomly sample  $N = 100$  individual EV flexibility sets according to the parameters specified in Table I (setting the heterogeneity parameter  $\sigma$  equal to one). Using these randomly sampled sets, we construct a structure-preserving outer approximation as a dilation of the base set given by  $\mathbb{Q} = N\mathbb{U}_0$ ; and compute a structure-preserving inner approximation  $\mathbb{P} = \bar{p} + \alpha\mathbb{U}_0$  by solving the LP in (22).

In Fig. 5, we plot the boundaries associated with the resulting inner and outer approximations of the aggregate flexibility set as solid-black lines and dotted-black lines, respectively. While the inner and outer approximations appear to be in close agreement, there is a noticeable difference between the two sets. This discrepancy is due to the conservatism of the approximation methods arising when there is heterogeneity between the individual flexibility sets. In Section V-C, we investigate the effect of heterogeneity on the approximation accuracy of our methods in more detail.

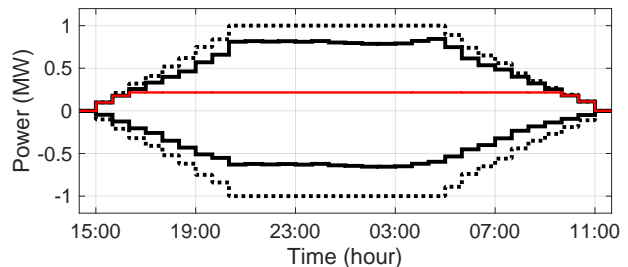
In Fig. 5(b), we also plot the aggregate charging profile  $u \in \mathbb{P}$  that minimizes peak aggregate power  $\|u\|_\infty$  (drawn as a solid red line). Fig. 5(a) depicts the corresponding net energy profile (drawn as a solid red line). The aggregate power profile  $u$  is disaggregated into individual charging profiles according to Eq. (30). For illustrative purposes, the individual power profiles are divided into five disjoint groups of 20 EVs each based on their order of arrival. The individual charging profiles within each group are summed and plotted in Fig. 5(c). Notice that the first group of EVs to arrive (represented by the red line) are charged at a high power level initially. But as more EVs arrive, their charging power levels decrease to ensure that the total aggregate power is minimized.

### C. Comparison of Inner Approximation Methods

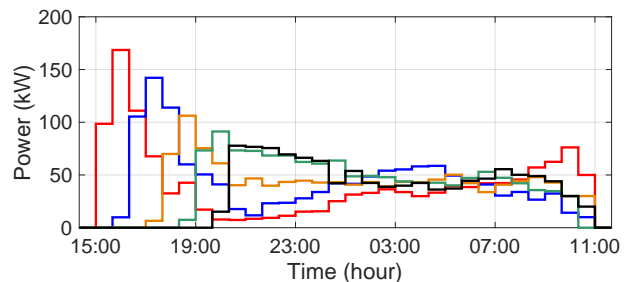
In this section, we examine the effect of heterogeneity between the individual flexibility sets on the approximation



(a) Aggregate net energy constraints



(b) Aggregate power constraints



(c) Partially disaggregated power profiles in groups of 20 EVs each

Fig. 5: Example of a structure-preserving inner approximation (solid-black line) and outer approximation (dotted-black line) of an aggregate flexibility set for  $N = 100$  EVs. The inner approximation  $\mathbb{P}$  is computed by solving the LP (22) and the outer approximation is computed according to  $\mathbb{Q} = N\mathbb{U}_0$ . Also depicted are: (b) an aggregate charging profile  $u \in \mathbb{P}$  that minimizes peak aggregate power (solid red line), (a) the corresponding net energy profile (solid red line), and (c) a partial disaggregation of the aggregate charging profile across five disjoint groups of 20 EVs each. The partially disaggregated charging profiles are grouped by order of arrival (e.g., solid red line corresponds to first 20 EVs, solid blue line corresponds to the next 20 EVs, etc.).

accuracy of three different inner approximation methods: those based on (i) general affine transformations computed according to (25), (ii) structure-preserving affine transformations computed according to (22), and (iii) structure-preserving homothetic transformations proposed by Zhao *et al.* [18] and computed according to (23).

As discussed in Remark 1, the method in [18] requires that  $\dim \mathbb{U}_i \geq \dim \mathbb{U}_0$  for all  $i \in \mathcal{N}$ . In the context of the EV charging model considered in this paper, this corresponds to a requirement that all EVs have identical arrival and departure times. Thus, for the purposes of this comparison, we assume

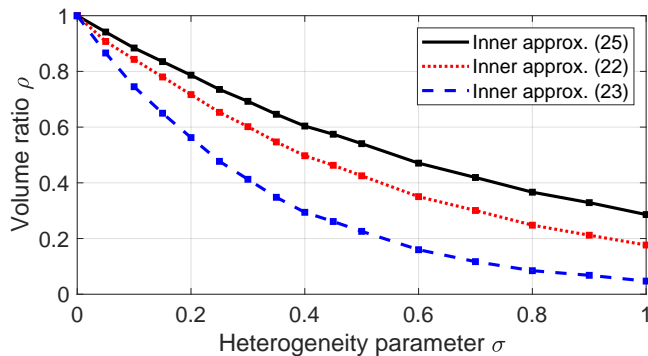


Fig. 6: Empirical average of the volume ratio  $\rho(\mathbb{P}, \mathbb{Q})$  versus the heterogeneity parameter  $\sigma$  for three different inner approximation methods.

that  $a_i = 0$  and  $d_i = T - 1$  for all  $i \in \mathcal{N}$ .

In comparing the different approximation methods, we vary the heterogeneity parameter  $\sigma$  from zero to one. Note that  $\sigma = 0$  corresponds to the special setting in which the individual flexibility sets are identical. For each value of  $\sigma$  considered, we conduct 300 independent experiments. For each experiment, we randomly sample  $N = 15$  individual flexibility sets. Given the sampled sets, we compute inner approximations to their aggregate flexibility set using each of the aforementioned methods. We then compute an outer approximation to their aggregate flexibility set by solving the LP in (37). Using the resulting outer approximation, we compute the volume ratio in Eq. (10) for each of the inner approximations. In Fig. 6, we plot the empirical average of the resulting volume ratios as a function of the heterogeneity parameter  $\sigma$  for each method.

For  $\sigma = 0$ , the average volume ratio equals one for all of the approximation methods considered, confirming that each method is able to recover the true aggregate flexibility set when the underlying individual flexibility sets are identical. While the performance of each method degrades as the degree of heterogeneity between the individual flexibility sets increases, both of the methods proposed in this paper are observed to strictly outperform the method in [18] for all values of  $\sigma > 0$ .

## VI. CONCLUSION

In this paper, we presented novel convex optimization methods to compute maximum-volume inner approximations and minimum-volume outer approximations of the Minkowski sum of heterogeneous EV flexibility sets. By restricting the class of approximating sets to those which can be expressed as affine transformations of a given convex polytope (termed the base set), we showed how to conservatively approximate the resulting optimization problems as linear programs that scale polynomially with the number and dimension of the individual flexibility sets. The proposed class of approximation methods were shown to generalize and improve upon the approximation accuracy of related methods in the literature. Our experiments also show that

the proposed approximations improve in accuracy as the individual flexibility sets become more homogeneous in nature, exactly recovering the aggregate flexibility set when the individual flexibility sets are identical. Finally, as a direction for future research, we intend to generalize the methods developed in this paper to incorporate more realistic EV charging models that account for charging inefficiencies and losses.

## REFERENCES

- [1] P. Alexeenko and E. Bitar, "Achieving reliable coordination of residential plug-in electric vehicle charging: A pilot study," *arXiv preprint arXiv:2112.04559*, 2021.
- [2] M. Muratori, "Impact of uncoordinated plug-in EV charging on residential power demand," *Nature Energy*, vol. 3, no. 3, pp. 193–201, 2018.
- [3] J. Quiros-Tortos, L. Ochoa, and T. Butler, "How electric vehicles and the grid work together: Lessons learned from one of the largest electric vehicle trials in the world," *IEEE Power and Energy Magazine*, vol. 16, no. 6, pp. 64–76, 2018.
- [4] Z. J. Lee, T. Li, and S. H. Low, "ACN-Data: Analysis and applications of an open EV charging dataset," in *Proceedings of 10th ACM International Conf. on Future Energy Systems*, 2019, pp. 139–149.
- [5] J. G. Smart and S. D. Salisbury, "Plugged in: How americans charge their electric vehicles," Idaho National Lab.(INL), Idaho Falls, ID (United States), Tech. Rep., 2015.
- [6] J. Bauman, M. Stevens, S. Hacıkyan, L. Tremblay, E. Mallia, and C. Mendes, "Residential smart-charging pilot program in Toronto: results of a utility controlled charging pilot," *World Electric Vehicle Journal*, vol. 8, no. 2, pp. 531–542, 2016.
- [7] B. Satchidanandan and M. A. Dahleh, "Economic dispatch for ev energy storage-integrated power systems," in *2022 14th International Conference on COMMunication Systems & NETWORKS (COMSNETS)*. IEEE, 2022, pp. 707–715.
- [8] "FERC Order No. 2222: Fact Sheet," [Online]. Available: <https://www.ferc.gov/media/ferc-order-no-2222-fact-sheet>.
- [9] R. Henríquez, G. Wenzel, D. E. Olivares, and M. Negrete-Pincetic, "Participation of demand response aggregators in electricity markets: Optimal portfolio management," *IEEE Transactions on Smart Grid*, vol. 9, no. 5, pp. 4861–4871, 2017.
- [10] "NYISO Compliance Filing Order No. 2222," [Online]. Available: <https://nyisoviewer.etariff.biz/ViewerDocLibrary//Filing/Filing1805/Attachments/20210719%20NYISO%20CmplncFlnng%20Order%20No.%202222.pdf>.
- [11] "California ISO Tariff Section 30 - Bid and Self-Schedule Submission in California ISO Markets as of Jan 1, 2022," [Online]. Available: <http://www.caiso.com/Documents/Section30-Bid-and-Self-ScheduleSubmission-in-CaliforniaISOMarkets-asof-Jan1-2022.pdf>.
- [12] P. Gritzmann and B. Sturmfels, "Minkowski addition of polytopes: computational complexity and applications to gröbner bases," *SIAM Journal on Discrete Mathematics*, vol. 6, no. 2, pp. 246–269, 1993.
- [13] K. Trangbaek and J. Bendtsen, "Exact constraint aggregation with applications to smart grids and resource distribution," in *2012 IEEE 51st IEEE Conference on Decision and Control (CDC)*. IEEE, 2012, pp. 4181–4186.
- [14] M. Alizadeh, A. Scaglione, A. Goldsmith, and G. Kesidis, "Capturing aggregate flexibility in demand response," in *53rd IEEE conference on decision and control*. IEEE, 2014, pp. 6439–6445.
- [15] S. Barot and J. A. Taylor, "A concise, approximate representation of a collection of loads described by polytopes," *International Journal of Electrical Power & Energy Systems*, vol. 84, pp. 55–63, 2017.
- [16] A. Nayyar, J. Taylor, A. Subramanian, K. Poolla, and P. Varaiya, "Aggregate flexibility of a collection of loads," in *52nd IEEE Conference on Decision and Control*. IEEE, 2013, pp. 5600–5607.
- [17] H. Hao, B. M. Sanandaji, K. Poolla, and T. L. Vincent, "Aggregate flexibility of thermostatically controlled loads," *IEEE Transactions on Power Systems*, vol. 30, no. 1, pp. 189–198, 2014.
- [18] L. Zhao, W. Zhang, H. Hao, and K. Kalsi, "A geometric approach to aggregate flexibility modeling of thermostatically controlled loads," *IEEE Trans. on Power Systems*, vol. 32, no. 6, pp. 4721–4731, 2017.

- [19] D. Madjidian, M. Roozbehani, and M. A. Dahleh, "Energy storage from aggregate deferrable demand: Fundamental trade-offs and scheduling policies," *IEEE Transactions on Power Systems*, vol. 33, no. 4, pp. 3573–3586, 2017.
- [20] F. L. Müller, O. Sundström, J. Szabó, and J. Lygeros, "Aggregation of energetic flexibility using zonotopes," in *2015 54th IEEE Conference on Decision and Control (CDC)*. IEEE, 2015, pp. 6564–6569.
- [21] F. L. Müller, J. Szabó, O. Sundström, and J. Lygeros, "Aggregation and disaggregation of energetic flexibility from distributed energy resources," *IEEE Trans. on Smart Grid*, vol. 10, no. 2, pp. 1205–1214, 2017.
- [22] M. S. Nazir, I. A. Hiskens, A. Bernstein, and E. Dall'Anese, "Inner approximation of minkowski sums: A union-based approach and applications to aggregated energy resources," in *2018 IEEE Conference on Decision and Control (CDC)*. IEEE, 2018, pp. 5708–5715.
- [23] S. Kundu, K. Kalsi, and S. Backhaus, "Approximating flexibility in distributed energy resources: A geometric approach," in *2018 Power Systems Computation Conference (PSCC)*. IEEE, 2018, pp. 1–7.
- [24] H. Hao and W. Chen, "Characterizing flexibility of an aggregation of deferrable loads," in *53rd IEEE Conference on Decision and Control*. IEEE, 2014, pp. 4059–4064.
- [25] L. Zhao, H. Hao, and W. Zhang, "Extracting flexibility of heterogeneous deferrable loads via polytopic projection approximation," in *IEEE 55th Conf. on Decision and Control*, 2016, pp. 6651–6656.
- [26] K. Hreinsson, A. Scaglione, M. Alizadeh, and Y. Chen, "New insights from the shapley-folkman lemma on dispatchable demand in energy markets," *IEEE Transactions on Power Systems*, vol. 36, no. 5, pp. 4028–4041, 2021.
- [27] S. Taheri, V. Kekatos, H. Veeramachaneni, and B. Zhang, "Data-driven modeling of aggregate flexibility under uncertain and non-convex load models," *arXiv preprint arXiv:2201.11952*, 2022.
- [28] B. Biegel, L. H. Hansen, P. Andersen, and J. Stoustrup, "Primary control by on/off demand-side devices," *IEEE Transactions on Smart Grid*, vol. 4, no. 4, pp. 2061–2071, 2013.
- [29] J. Mathieu, S. Koch, and D. Callaway, "State estimation and control of electric loads to manage real-time energy imbalance," *Power Systems, IEEE Transactions on*, vol. 28, pp. 430–440, 02 2013.
- [30] H. Hao, Y. Lin, A. Kowli, P. Barooah, and S. Meyn, "Ancillary service to the grid through control of fans in commercial building hvac systems," *IEEE Trans. Smart Grid*, vol. 5, pp. 2066–2074, 2014.
- [31] S. Meyn, P. Barooah, A. Busic, Y. Chen, and J. Ehren, "Ancillary service to the grid using intelligent deferrable loads," *IEEE Transactions on Automatic Control*, vol. To appear, 12 2014.
- [32] Z. J. Lee, G. Lee, T. Lee, C. Jin, R. Lee, Z. Low, D. Chang, C. Ortega, and S. H. Low, "Adaptive charging networks: A framework for smart electric vehicle charging," *IEEE Transactions on Smart Grid*, vol. 12, no. 5, pp. 4339–4350, 2021.
- [33] H. R. Tiwary, "On the hardness of computing intersection, union and minkowski sum of polytopes," *Discrete & Computational Geometry*, vol. 40, no. 3, pp. 469–479, 2008.
- [34] S. Sadraddini and R. Tedrake, "Linear encodings for polytope containment problems," in *2019 IEEE 58th Conference on Decision and Control (CDC)*. IEEE, 2019, pp. 4367–4372.
- [35] M. E. Dyer and A. M. Frieze, "On the complexity of computing the volume of a polyhedron," *SIAM Journal on Computing*, vol. 17, no. 5, pp. 967–974, 1988.
- [36] K. Kellner, "Containment problems for projections of polyhedra and spectrahedra," *arXiv preprint arXiv:1509.02735*, 2015.
- [37] S. V. Raković, E. C. Kerrigan, D. Q. Mayne, and K. I. Kouramas, "Optimized robust control invariance for linear discrete-time systems: Theoretical foundations," *Automatica*, vol. 43, no. 5, pp. 831–841, 2007.
- [38] J. M. Ortega and W. C. Rheinboldt, *Iterative solution of nonlinear equations in several variables*. SIAM, 2000.
- [39] S. Boyd, S. P. Boyd, and L. Vandenberghe, *Convex optimization*. Cambridge university press, 2004.